DIGITAL ARRAY MIMO RADAR AND ITS PERFORMANCE ANALYSIS

N. B. Sinha

Faculty of Electronics and Communication Engineering and
Electronics and Instrumentation Engineering
College of Engineering & Management Kolaghat
Purba-Medinipur, West Bengal 721171, India

R. Bera

Faculty of Electronics and Telecommunication Engineering
Sikkim Manipal Institute of Technology
Sikkim Manipal University
Majitar, Sikkim 737132, India

M. Mitra

Faculty of Electronics and Telecommunication Engineering
Bengal Engineering and Science University
Shibpur, Howrah-11103, India

Abstract—In this paper we formalizes a new discrete time model of digital array based MIMO radar in which the combined effects of the transmit filter, physical MIMO multi-path channel fading, and receive filter. It has the same sampling period as that of the MIMO receiver. Apart from this, SNR value and target detection are different in compared to the continuous domain nature. Orthogonality is introduced using OSTBC (orthogonal space time coding) including interelement spacing at the transmitter is greater than the target beam width coverage. For space and temporal diversity we have considered distributed source model. and modulation schemes respectively. Frequency diversity is achieved using N point IFFT ($N = 32$, 64, 256, 1024) at the base band. Thus, three dimensional analysis with respect to diversity and selective nature of fading channel in digital array based MIMO radar are now used for performance analysis based on probability of detection, symbol error rate, model error, power spectral density at the receiver and SNR value at the detector.

1. INTRODUCTION

It has been recently shown that multiple-input multiple-output (MIMO) [1, 2] antenna systems have the potential to dramatically improve the performance of communication systems over single antenna systems. Unlike beam forming, which presumes a high correlation between signals either transmitted or received by an array, the MIMO concept exploits the independence between signals at the array elements. In conventional radar, target scintillations are regarded as a nuisance parameter that degrades radar performance. The novelty of MIMO radar is that it takes the opposite view, namely, it capitalizes on target scintillations to improve the radar's performance. The MIMO radar system under consideration consists of a transmit array with widely-spaced elements such that each views a different aspect of the target. It can overcome target RCS scintillations by transmitting different signals from several decor related transmitters. The received signal is a superposition of independently faded signals, and the average SNR of the received signal is more or less constant. This is in marked contrast to conventional radar, which under classical Swelling models suffers from large variations in the received power. Therefore the objectives of MIMO radar are the target resolution should have the higher as compared to conventional radar. Interference and clutter rejection should be the highest, RCS measurement accuracy should be the highest and multi-path and other environmental effects should be the minimum. But unfortunately MIMO technology alone cannot tackle all the problems solution.

With the rapid growth of MIMO Technology for wireless application and easy availability of several books on 'Smart Antennas' [17–19], a trend is noticed for the development of MIMO radar for smart car(Intelligent Transport System) ITS application. The fundamental temporal time or frequency domain processing in the form of Doppler range/MTI are updated with space domain processing resulting in (Space time Processing) STP. Putting multiple antennas both at transmitter and receiver along with (Direction of arrival) DOA estimation and then antenna pattern synthesis (adaptive beam forming), the antenna beam may be focused to a particular targets. A multiple access in the form of SDMA can be thought of, for multiple targets detection and information using STAP/MIMO. DSP algorithms are smart enough to enable above mentioned technology with the result of improved target detection buried in clutter, interference and multi path condition. Considering the poor signal conditions at the radar receiver, authors are prompted to develop MIMO radar for Car collision avoidance.

Some notational conventions are:

* Lower case letters denote scalars, upper case letters denote matrices and boldface denote vectors.
* Subscript $(\cent)H$ denotes Hermitian transpose.
* The operator $E(\cent)$ denotes expectation.
* The operator $k(\cent)$ denotes matrix norm.
* The operator $l\max(\cent;\cent)$ denotes the largest generalized eigenvalue of a pair of matrices.
* Let w be a beam forming weight vector. Then wli denotes the beam forming weight vector of the ith user in the lth iteration.
* The operator $P(\cent)$ returns the principal eigenvector of a matrix, that is the eigenvector corresponding to its maximal eigenvalue.

2. MIMO CHANNEL DESCRIPTION

In quasi-static, independent and identically distributed (i.i.d.) frequency flat Rayleigh fading channels, MIMO target detection probability and receiver SNR increases as the number of antennas increases. This has been discussed in detail in later half as space diversity. In general, the sub channels of MIMO radar system are usually space selective because of the angle spread at the transmitter and/or receiver. Consider the multistatic nature of the radar where orthogonality is maintained in space domain using the condition

$$(D_t * D_r)/R > \lambda/M \tag{1}$$

where D_t and D_r are the transmit and receive antenna spacing, R is the range between transmitter and receiver, λ is the wavelength, M is the number of transmit antennas (assume that M is large). In practice, for larger values of antenna spacing (1) the transmit antennas can fall into the grating lobes of the receive array, in this case, orthogonality is not realized. In a pure LOS situation, orthogonality can only be achieved for very small values of range R. This makes the DOD (Direction of departure) at the transmitter and DOA (Direction of arrival) at the receiver end uncorrelated. This makes the receiver robust against clutters and multipath effects. In other words, this is known as space diversity.The time-selective nature is caused by the Doppler spread and the frequency selective nature is caused by delay spread. The element $h_{p,q}$ of the channel matrix provides the complex valued channel gain from transmitter antenna p to receiver antenna q. Let $h_r(t)$ and $h_t(t)$ the time-invariant impulse responses of the transmit filter and the receive filter, respectively, and both are normalized with energy

of unity. Let $H_t(t, f)$ be the time-variant frequency responses for the channel before hitting the target and $H_r(t, f)$ be the time-variant frequency responses for the channel before hitting the receiver. Using the distances and the coordinates of the target in spherical coordinates can be written as

$$H_t(t, f) = [(1/|r_1|)] * \left[e^{j(\omega t - kr)} \right] \text{ and } H_r(t, f) = [(\sigma/|r_2|)] * \left[e^{j(\omega t - kr)} \right],$$

where $\omega = 2\pi f$ is the angular frequency of the transmitted signal and t is the time taken for the signal to reach the target from the transmitter, $k = 2\pi(\sin\theta(\cos\phi)i + (\sin\theta*\sin\varphi)j + \cos\varphi)$ is the freespace wavenumber of the signal and where σ is the target reflectivity (which depends upon the receive look angles, θ the elevation and Φ, the azimuth). For simplicity one-dimensional ULAs of antennas with antenna spacing d_t and d_r. The channel matrix can be described the array steering and response vectors given by

$$a_T(\theta_T) = \frac{1}{\sqrt{P}} \left[1, e^{-j2\Pi\theta_T}, \dots e^{-j2\Pi(P-1)\theta_T} \right]^T$$

$$a_R(\theta_T) = \frac{1}{\sqrt{Q}} \left[1, e^{-j2\Pi\theta_R}, \dots e^{-j2\Pi(Q-1)\theta_R} \right]^T$$

Let $g_{m,n}(t, \tau)$ be the time-varying impulse response of the (m, n)th sub-channel connecting the mth transmit antenna and the nth receive antenna. Hence, $g_{m,n}(t, \tau) = [\sigma/\text{mod}(r1) * \text{mod}(r2)] * [e^{j(w-\tau)-k(r1+r2)}] * a_T(\theta_T) * a_R(\theta_R)$. The complete channel matrix just before reaching the receiver is given $H_{m,n}(t, \tau) = g_{m,n}(t, \tau) * h_r(\tau) * h_t(\tau)$.

The above relation is based on Kronecker product. Let $s_n(k)$ is a sequence of complex symbols of OSTBC transmitted by the nth transmit antenna with symbol period of $y_m(t)$ is the received signal at the mth receive antenna, and $y_m(k)$ is the sampled version of $y_m(t)$ with sampling period of $T_s = Tsym/\gamma$, and γ is an integer number. If $\gamma = t$, then the sampling rate at the receiver is the same as the symbol rate at the transmitter. Using the time-frequency duality and convolution operation, the received signal can be finally represented as

$$y_m(t) = \sum_{n=1}^{N} \sum_{k=-\infty}^{\infty} s_n(k)h_{m,n}(t, t - kT_{sym}) + z_m(t), \quad \text{where, } m = 1, 2, 3$$

and the additive noise given by

$$z_m(t) = v_m(t) \otimes P_R(t) \tag{2}$$

and $v_m(t)$ is the zero-mean complex-valued white Gaussian noise with a two-sided power spectral density $P_R(t) = P_T(t)$. The sampled version of the received signal at the qth receive antenna is given

$$y_m(kT_s) = \sum_{n=1}^{N} \sum_{t=-\infty}^{\infty} s_n(l)h_{m,n}(KT_s, KT_s - l\gamma T_s) + z_m(KT_s),$$

$$\text{where} \quad m = 1, 2, \ldots M \tag{3}$$

If we over sample the transmitted sequence $s_n\{k\}$ by inserting zeros between each $\{\gamma - 1\}$ symbol $s_n\{k\}$, then the over sampled sequence $x_n(K)$ can be defined as

$$x_n(K) = \begin{array}{ll} s_n\left(\dfrac{k}{\gamma}\right), & \text{if } \left(\dfrac{k}{\gamma}\right) \text{ is integer} \\ 0 & \text{otherwise.} \end{array} \tag{4}$$

The signal vector received by the MIMO radar (after demodulation and matched filtering) is given by

$$y_m(k) = \sum_{n=1}^{N} \sum_{k=-\infty}^{\infty} x_n(k-1)h_{m,n}(k,l) + z_m(k),$$

$$\text{where} \quad m = 1, 2, 3, \ldots M \tag{5}$$

where $h_{m,n}(k,l) = h_{m,n}(kTs, lTs)$ and Ts is the sampled version of $h_{m,n}(t, \tau)$ and $z_m(k) = zm(kTs)$ where Ts is the sampled version of $z(t)$. With the statistical properties of the discrete-time channel coefficients $h_{m,n}(k,l)$ and the additive noises $z_m(k)$, the MIMO channel input-output can be fully characterized in the discrete time domain with high computational efficiency and no loss of information.

3. MIMO CHANNEL ASSUMPTIONS

Assumptions for the continuous-time physical channel of wideband MIMO wireless systems are as follows:

Assumption 1: The (p,q)th sub channel of $g_{m,n}(t, \tau)$ a MIMO system is a wide-sense stationary uncorrelated scattering (WSSUS) [15, 16] rayleigh fading channel with a zero mean and autocorrelation given by

$$E\left\{g_{m,n}(t,\tau) * g_{m,n}^*\left(t - \xi, T'\right)\right\} = J_0\left(2\Pi f_d\xi\right) * G(\tau) * \delta\left(T - T'\right), \ \forall_{m,n} \tag{6}$$

where $(.)^*$ is the conjugate operator d is the maximum Doppler frequency, and $G(\Gamma)$ is the power delay profile with $\int_{-\infty}^{\infty} G(\tau)d\tau = 1$, where

$$G(\tau) = \sum_{i=1}^{K} \sigma_i^2 \delta(\tau - \tau_i) \tag{7}$$

where k is the number of total resolvable paths and σ is the power of the ith path with delay Γ. For example in wireless communication, the typical urban (TU), hilly terrain (HT), and equalization test (EQ) pro-files for GSM and EDGE systems [7] as well as the pedestrian and vehicular profiles for channel A and channel B of cdma2000 and UMTS systems [8] have all been defined as discrete delayed Rayleigh fading paths, and almost all the path delays are not an integer multiple of their system's symbol period domain. These statistics are further used to build a computationally efficient discrete-time MIMO channel simulator which is equivalent to its counterpart in the continuous-time domain in terms of various statistic measures.

Assumption 2: The space selectivity or (spatial correlation) between the (m, n)th subchannel $H_{m,n}(t, T)$ and the (p, q)th subchannel $H_{p,q}(t, T)$ is given by

$$E\left\{ H_{m,n}(t, \tau) * H_{p,q}^* \left(t - \xi, T^{/} \right) \right\}$$
$$= \rho_{RX}^{(m,p)} * \rho_{TX}^{(n,q)} * J_0 \left(2\Pi f_d \xi \right) * G(\tau) 8\delta \left(T - T^{/} \right), \tag{8}$$

where $\rho_{RX}^{(m,p)}$ is the receiver correlation Coefficient between receive antennas m and p with $0 =< \text{abs}(\rho_{RX}^{(m,p)}) =< \rho_{RX}^{(m,p)} = 1$, and $\rho_{TX}^{(n,q)}$ is the transmitter correlation Coefficient between receive antennas n and q with $0 =< \text{abs}\rho_{TX}^{(n,q)} =< \rho_{TX}^{(n,q)} = 1$. Assumption 2 is a straightforward extension of the MIMO Rayleigh flat fading [9] to the MIMO WSSUS multipath Rayleigh fading case. It implies three sub assumptions. The transmit correlation between the fading from transmit antennas and to the same receive antenna does not depend on the receive antenna. The receive correlation between the fading from a transmit antenna to receive antennas and does not depend on the transmit antenna and the correlation between the fading of two distinct transmit-receive antenna pairs is the product of the corresponding transmit correlation and receive correlation. These three sub assumptions are actually the "Kronecker correlation" assumption used in the literature, and they are quite accurate and commonly used for MIMO rayleigh

fading channels [6, 10]. However, it should be pointed out that the third sub assumption may not be extended to Rayleigh fading MIMO channels [11]. Spatial correlation coefficients are determined by the spatial arrangements of the transmit and receive antennas, the angle of arrival, the angular spread, etc. This can be calculated by mathematical formulas (6), (10) or obtained from experimental data.

4. DISCRETE-TIME MIMO CHANNEL MODEL FOR MIMO RADAR

4.1. Discrete Time Channel Model

This discrete-time model based on MIMO Rayleigh fading channels and investigate the statistical properties of this MIMO channel in the discrete-time domain. These statistics are further used to build a computationally efficient discrete-time MIMO channel simulator, which is equivalent to its counterpart in the continuous-time domain in terms of various statistic measures depicted in Fig. 1.
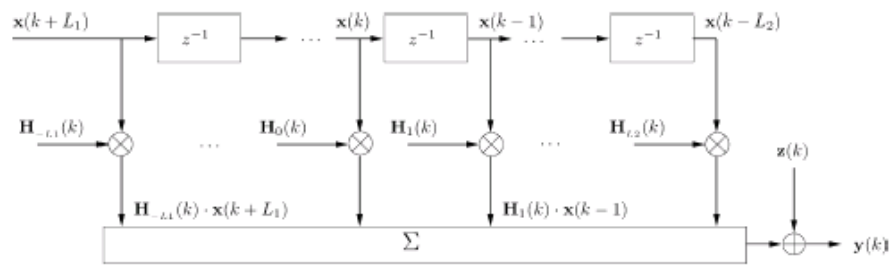
Figure 1. Discrete time model in 3D processing of MIMO radar.

It is known that the total number of spaced discrete-time channel coefficients is determined by the maximum delay spread of the physical fading channel and the time durations of the transmit filter and receive filter which are usually infinite in theory to maintain limited frequency bandwidth. Therefore, it is normally a time-varying noncausal filter with infinite impulse response (IIR). However, in practice, the time-domain tails of the transmit and receive filters are designed to fall off rapidly. Thus, the amplitudes of the channel coefficients will decrease quickly. When the power (or squared amplitude) of a coefficient is smaller than a predefined threshold, for example, 0.01% of the total power of its corresponding sub channel, it has very little impact on the output signal and thus can be discarded. Therefore, the time-varying noncausal IIR channel can be truncated to a finite impulse

response (FIR) channel. Without loss of generality, we assume that the coefficient index l is in the range of $[-L_1, L_2]$, where L_1 and L_2 are nonnegative integers, and the total number of coefficients for the truncated FIR channel $h_{m,n}(k, L)$ is L with $L <= L_1 + L_2$, where the equality is held if there are no discarded coefficients within the coefficient index range of $(-L_1, L_2)$. Based on the above discussion and (6) the input-output relationship of the MIMO channel in the discrete- time domain as follows:

$$y(K) = \sum_{l=-L_1}^{L_2} H_l(K) \cdot X(K - l) + Z(K) \qquad (9)$$

where

$$\begin{aligned} X(K) &= [x_1(k), x_2(k), \dots, x_n(k)]^t \\ Z(k) &= [z_1(k), z_2(k), \dots, z_n(k)]^t \\ Y(k) &= [y_1(k), y_2(k), \dots, y_n(k)]^t \end{aligned}$$

are the input vectors, noise vectors, and output vectors at the time instant k, respectively with $(.)^t$ represents transpose operator; $H_l(K)$ is the LT_s delayed channel matrix at time instant k and defined by

$$H_l(K) = \begin{bmatrix} h_{1,1}(K,l) & \cdots & h_{1,N(K,l)} \\ \vdots & \ddots & \vdots \\ h_{M,1}(k,l) & \cdots & h_{M,N}(K,I) \end{bmatrix}$$

It is noted that there are (MNL) stochastic channel coefficients, and an-element random noise vector in this MIMO Rayleigh fading model (10). Since all of them are complex valued Gaussian random variables, the first-order and second order statistics of the channel coefficients and the noise vector will be sufficient to fully characterize the MIMO channel. For the convenience of discussion, we define the MIMO channel coefficient vector

$$h_{vcc(k)} = \{[h_{1,1}(k), h_{1,2}(k), \dots h_{1,N}(k)] \dots [h_{M,1}(k), h_{M,2}(k), \dots h_{M,N}(k)]\}^t$$

where $h_{M,N}(k)$ is the (m, n)th sub channel's FIR coefficients at time k given by

$$h_{M,N}(k) = [h_{M,N}(k, L_1) \dots h_{1M,N}(k, L_2)] \qquad (10)$$

We are now ready to discuss the statistical properties of the MIMO channel.

With the statistical properties of the discrete-time channel coefficients and the additive noises (including clutter, multipath effect and uncorrelated fading), the MIMO channel input-output can be fully characterized in the discrete time domain with high computational efficiency and no loss of information. It gives a deep insight into channel distortions caused by scattering components with different propagation delays $k^/$ and discrete frequencies $f_n \cdot f_n^/ = f_n$ when considering two dimensional discrete time Fourier transform of $s(k^/, f_n)$.

In this case the four correlation functions $h(k^/, k)$, $H(k^/, k)$, $s(k^/, f_n)$, $T(f_n^/, f_n)$ are stochastic system functions representing discrete time impulse response, discrete time Transfer function, discrete time Doppler variant impulse response, discrete time Doppler variant transfer function. Generally, these stochastic system functions are described by the following autocorrelation functions:

$$r_{hh}\left(k_1^/, k_2^/; k_1, k_2\right) := E\left\{h * \left(k_1^/, k_1\right) h \left(k_2^/, k_2\right)\right\},$$

$$r_{HH}\left(f_{n1}^/, f_{2n}^/; k_1, k_2\right) := E\left\{H * \left(f_{n1}^/, k_1\right) H \left(f_{2n}^/, k_2\right)\right\},$$

$$r_{ss}\left(k_1^/, k_2^/; f_{n1}, f_{n2}\right) := E\left\{s * \left(k_1^/, f_{n1}\right) s \left(k_2^/, f_{n2}\right)\right\},$$

$$r_{TT}\left(f_{n1}^/, f_{n2}^/; f_{n1}, f_{n2}\right) := E\left\{T * \left(f_{n1}^/, f_{n1}\right) T \left(f_{n2}^/, f_{n2}\right)\right\},$$

In case of WSSUS (wide sense stationary uncorrelated scattering), the time difference $(t_2 - t_1)$ in discrete domain is $(K_2 - K_1) := K$ as such $r_{hh}(k_1^/, k_2^/; k_1, k_1 + k) = \delta(k'2 - k'1)S_{hh}(k_1^/, k)$, where $S_{hh}(k_1^/, k)$ is called delayed cross-power spectral density. With this representation it becomes obvious that discrete time-variant impulse response $h(k^/, k)$ of WSSUS models has the characteristic properties of non-stationary white noise,clutter, multipath with respect to propagation delay $K^/$, on the one hand, it is also stationary with respect to the time k, on the other hand. By analogy directly obtain autocorrelation function of $T(f_n^/, f_n)$. $r_{TT}(f^/, f^/ + v^/; f^1, f^2) = \delta(f_2 - f_1)S_{TT}(v^/, f_1)$, where $V_1 = f_{n2} - f_{n1}$ and $S_{TT}(f_{n1}^/, v_1)$ is called Doppler cross power spectral density.

5. MODEL ERROR

Figure 2 illustrates that the model error decreases if the sampling frequency (fs) increases. In this limit fs tending to infinity or sampling time tending to zero.
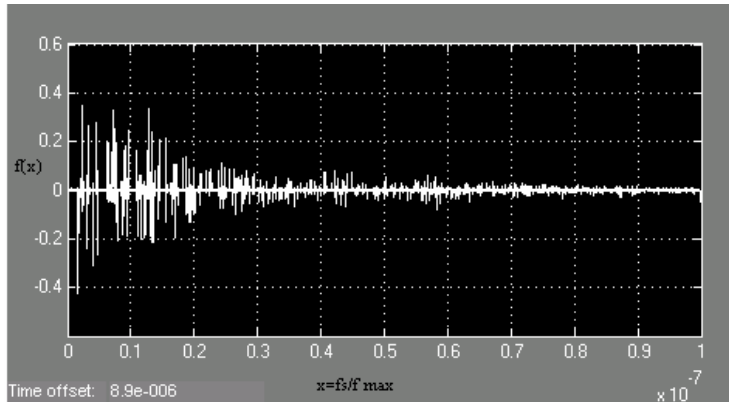
Figure 2. Represents the quantized frequencies, time and phase approaches continuous model.

6. MODEL COMPLEXITY

This section illustrate the measurement of the computational complexity and the complexity of our proposed discrete-time MIMO channel simulation model is much lower than that of the conventional continuous-time simulation model based on the following aspects. i) The sampling rate of the discrete-time model is equal to the small positive integer. However, for the conventional continuous-time model, when the differential delay of multiple fading paths is very small compared to the symbol period, the sampling rate for simulation needs to be very high to implement the multiple fading paths. Sampling rate for the continuous-time model is the sampling computational complexity ratio of the discrete-time model to the continuous-time models is given by

$$\xi_n = \frac{\eta}{\eta_c} \times 100\%$$

Therefore, the ratio between the number of operations of decomposing one large matrix and the number of operations Since is usually much larger than, the ratio is usually very small. For channels with continuous power delay profile, such as the exponential power delay profile [12], a much higher is required for continuous-time model, which will lead to an even smaller. ii) For the discrete-time model, the effects of the transmit and receive filters are incorporated in the statistical channel coefficients with no additional filtering calculations involved. However, the simulation of the continuous-time model must

pass the input signals through the transmit and receive filters with extra computations. Moreover, to represent the small differential delay of multiple fading paths, the continuous-time model has to use a high sampling rate which makes the transmit and receive filters have large number of taps. This makes the computational complexity of the continuous-time model even higher than that of the discrete-time model. Unfortunately, an explicit ratio between these two models is unlikely to be obtained.

7. RESULTS AND SIMULATIONS

7.1. Detection Performance

A useful measure of radar fidelity is probability of detection (PD). Analytical forms of PD are obtained using radar detection theory originally described by Woodward [12]. It is not always feasible, or even possible, to find closed forms expressions for PD for every kind of radar. The detection performance comparison of radars thus becomes intractable in some cases. However, in this paper, we have used an alternative way to gauge the fidelity of radars by postulating an analogous communication system for radars (ACSR). Effective SER for this system have been calculated. Simple radar topologies have been used in this paper (as described above) to find closed form expressions for both techniques and to compare their simulation results. This has helped to obtain the parallel between probability of miss-detection ($PMD = 1 - PD$) of a radar and SER of the ACSR, by plotting graphs of each of these quantities against the received signal-to-noise ratio (SNR) for every kind of radar under test.

7.1.1. Symbol Error Rate

Using this model, the 1×1 SISO radar has only one channel in the ACSR. The 2×1 MISO and the 1×2 SIMO radars have two channels each and the 2×2 MIMO radar has four channels. This leads to the expressions for the received signal-to-noise ratios (SNRs) of each of these radars in terms of the respective channels:

$$SNR_{SISO} = (|h_1|)^2 \frac{E_m}{\delta_n^2}$$

$$SNR_{MISO} = \frac{1}{2}(|h_1| + |h_2|)^2 \frac{E_m}{\delta_n^2}$$

$$SNR_{SIMO} = (|h_1| + |h_2|)^2 \frac{E_m}{\delta_n^2}$$

$$SNR_{MIMO} = 0.5(|h_1| + |h_2| + |h_3| + |h_4|)^2 \frac{E_m}{\delta_n^2}$$

where h_1, h_2, h_3, h_4 are the channels that are set-up in the respective ACSRs and E_m is the signal power while $2n$ is the noise power spectral density. Now the radars have been converted into communication systems. The SER of each of these systems is found using BPSK and QPSK modulation schemes. In BPSK with an additive white Gaussian noise (AWGN), the SER is given by $P_b = Q(\sqrt{\frac{2E_m}{\delta_n^2}})$, where $Q(x) = 1/2 erfc(x/1.414)$. The target can occupy any position in space defined by azimuth-elevation space $\theta = [0, pi]$ and Φ defined by $= [0, 2pi)$. Let $p(\theta, \Phi)$ be the probability density function of the target positions. Then the SERs of each of the four radar systems are given, using BPSK, by:

$$P_{SISO} = \int_0^{2\Pi} \int_0^{\Pi} Q\left(\sqrt{2(|h_1|)^2 \frac{E_b}{N_q}}\right) p(\theta, \varphi) \sin\theta d\theta d\varphi$$

$$P_{MISO} = \int_0^{2\Pi} \int_0^{\Pi} Q\left(\sqrt{(|h_1| + |h_2|)^2 \frac{E_b}{N_q}}\right) p(\theta, \varphi) \sin\theta d\theta d\varphi$$

$$P_{SIMO} = \int_0^{2\Pi} \int_0^{\Pi} Q\left(\sqrt{2(|h_1| + |h_2|)^2 \frac{E_b}{N_q}}\right) p(\theta, \varphi) \sin\theta d\theta d\varphi$$

$$P_{MIMO} = \int_0^{2\Pi} \int_0^{\Pi} Q\left(\sqrt{(|h_1| + |h_2| + |h_3| + |h_4|)^2 \frac{E_b}{N_q}}\right) p(\theta, \varphi) \sin\theta d\theta d\varphi$$

By assuming uniform probability distribution for the target and an arbitrary fading probability distribution for the radar target reflectivity over all the azimuth-elevation space, the integrals in the above equations are evaluated numerically. Fig. 4 shows the results of SER performances. For all SNR levels, MIMO system has the least SER, and hence the highest probability of detection because the lower the error in the received signals, the higher is the detection.

The results obtained from the Modeling and simulation of MIMO radar are encouraging which is being ported to the PC subsystem where XPC target RTOS based kernel is being used for the final implementation. performance analysis of the system in terms of Pmd, SER & PSD analysis curves are shown in Figs. 3, 4 & 6 respectively Both the Pmd & SER values are falling noticeably with more no of transmit and receive antennas. More interesting points to be noted from the curves are that, the PER and BER performances improve at lower values of PSK resulting in less complexity in system implementation in temporal domain. Of course, the SNR at the
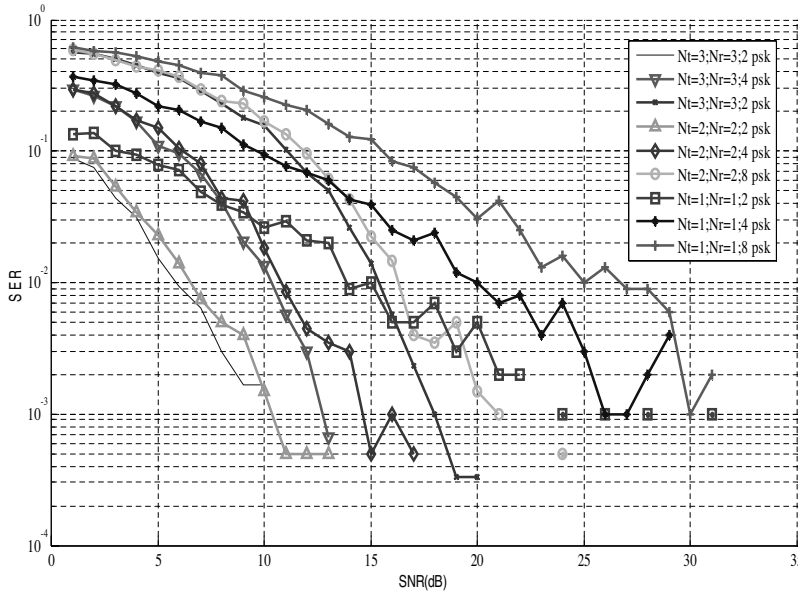
Figure 3. In discrete time model the symbol error rate is being calculated with respect to SNR value.
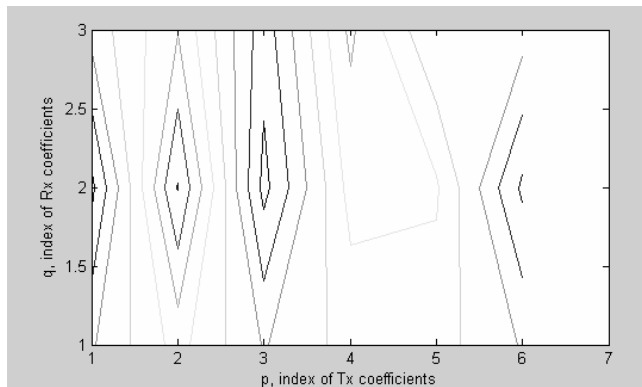
Figure 4. Channel coefficients for digital array 3 by 3 MIMO radar with respect to contour profile.

receiver degrade with lower PSK values but the outage probability will improve. The authors are expecting the improvement of both the channel capacity and the outage probability by having MIMO in their system implementation instead of STP. The contour plot determines the dependencies with respect to the time between the
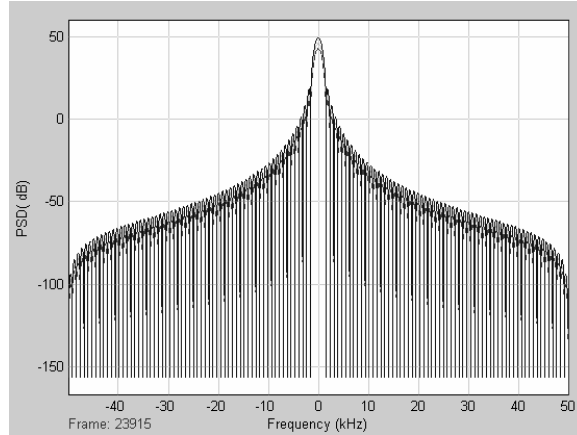
Figure 5. The power spectral density of the Discrete time digital array MIMO radar.
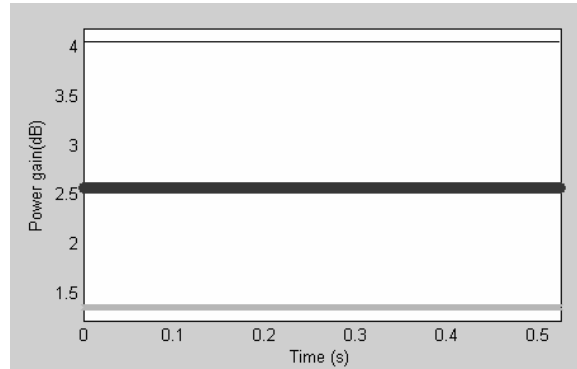
Figure 6. Dynamic variation in absolute power gain of the three parallel SISO channels.

channel coefficients of the discrete time MIMO channel.

The contour plot determines the dependencies with respect to the time between the channel coefficients of the discrete time MIMO channel.

7.1.2. PSD at the Receiver

Power spectral density at the receiver end considering the situation when the target is detected at the peak value of the spectral after demodulating and filtering. Here three by three antenna configuration

is used for MIMO radar test. Also the target is assumed to be modulating passive object. Thus, the space diversity is being taken into action to have better outlook with respect to multistatic radar.

7.1.3. Time Response of the Channel Coefficient of $3 * 3$ MIMO

The power level at the transmitter considering the multistatic nature of radar depending upon the position of the target based on SNR value at the receiver. The three parallel channels are notified which indicate that diversity in power is uniform with respect to gain level. Thus, individual antennas will behave in uncorrelated manner with respect to the orthogonality due to OSTBC and antenna spacing.

8. CONCLUSION

We have proposed a new discrete-time channel model for digital array based MIMO radar systems over space-selective (or spatially correlated), time-selective (or time-varying), and frequency-selective Rayleigh fading channels, which are referred to as triply selective Rayleigh fading channels. The stochastic channel coefficients of the new MIMO channel model have the same sampling period as that of the MIMO receiver, and they can be efficiently generated from a new method presented in this paper. The proposed approach combines the effects of the transmit filter, the physical MIMO channel multipath fading, and the receive filter. The new model is computationally efficient to describe the input-output of MIMO channels because it does not need to over sample the fractionally delayed multipath channel fading, the transmit filter, and the receive filter. It is shown through analysis and simulation that the discrete-time stochastic channel coefficients of different individual sub channels with different delays are generally *statistically correlated* even if the physical channels have WSSUS multipath fading. The knowledge of this correlation may be used for improving the channel estimation of MIMO systems. The statistical accuracy of the discrete-time channel model is rigorously confirmed by extensive simulations in terms of second-order statistics, probability of miss detection, and SER performance of a system that uses the model. The discrete-time MIMO channel model is further used to evaluate the MIMO channel capacity under a triply selective Rayleigh fading environment. For the high Pmd scenario, from the simulation experiments, we have two observations: • when the number of receive antennas is the same or constant as the number of transmit antennas the MIMO SNR at the receiver varying in a linear fashion, • when is fixed, the MIMO SNR at the receiver increases approximately

linearly. However, the scaling rates for all the three cases are dependent on the spatial correlation coefficients (the less correlation, the larger the scaling rate). This observations are therefore valuable extensions to the Shannon channel capacity results of triply selective MIMO Rayleigh fading channels from the special case of quasistatic i.i.d. flat Rayleigh fading MIMO channels in multistatic radar systems.

REFERENCES

1. Foschini, G. J., "Layered space-time architecture for wireless communication in a fading environment when using multiple antennas," *Bell Labs Technical Journal*, Vol. 1, 41–59, 1996.

2. Foschini, G. J. and M. J. Gans, "On the limits of wireless communications in a fading environment when using multiple antennas," *Wireless Pers. Commun.*, Vol. 6, 311–335, 1998.

3. Fishler, E., A. Haimovich, R. Blum, L. Cimini, D. Chizhik, and R. Valenzuela, "MIMO radar: An idea whose time has come," *Proc. of the IEEE Int. Conf. on Radar*, Philadelphia, PA, April 2004.

4. Fishler, E., A. Haimowich, R. Blum, L. Cimini, D. Chizhik, and R. Valenzuela, "Statistical MIMO radar," *12th Conf. in Adaptive Sensor Array Processing*, 2004.

5. Khan, H. A., D. J. Edwards, W. Q. Malik, and C. J. Stevens, "Ultra wideband multiple-input multiple-output radars," *IEEE International Radar Conference*, Arlington, Virginia, USA, 2005.

6. Johnson, D. and D. Dudgeon, *Array Signal Processing*, Prentice-Hall, Englewood Cliffs, NJ, 1993.

7. "Radio transmission and reception," ETSI. GSM 05.05, ETSI EN 300 910 V8.5.1, 2000.

8. "Selection procedure for the choice of radio transmission technologies of UMTS," UMTS, UMTS 30.03 version 3.2.0 ETSI, 1998.

9. Chuah, C. N., D. N. C. Tse, J. M. Kahn, and R. A. Valenzuela, "Capacity scaling in MIMOwireless systems under correlated fading," *IEEE Trans. Inform. Theory*, Vol. 48, 637–650, Mar. 2002.

10. Loyka, S. and A. Kouki, "New compound upper bound on MIMO channel capacity," *IEEE Commun. Lett.*, Vol. 6, 96–98, Mar. 2002.

11. Abdi, A. and M. Kaveh, "A space-time correlation model for multielement antenna systems in mobile fading channels," *IEEE J. Select. Areas Commun.*, Vol. 20, 550–560, Apr. 2002.

12. Jeruchim, M. C., P. Balaban, and K. S. Shanmugan, *Simulation of Communication Systems: Modeling, Methodology, and Techniques*, 2nd edition, Kluwer, Berlin, Germany, 2000.

13. Woodward, P. M., *Probability and Information Theory with Application to Radar*, Artech House, MA, 1953.

14. Xiao, C., et al., "A discrete-time model for triply selective MIMO rayleigh fading channels," *IEEE Transactions on Wireless Communications*, Vol. 3, No. 5, September 2004.

15. Bello, P. A., "Characterization of randomly time-variant linear channels," *IEEE Trans. Commun. Syst.*, Vol. 11, 360–393, Dec. 1963.

16. Parsons, J. D., *The Mobile Radio Propagation Channel*, 2nd edition, Wiley, New York, 2000.

17. Reed, J. H., "Software radio — A modern approach to radio engineering," *Smart Antenna*, Chapter 6, Pearson Education, 2006.

18. Sarkar, T. K., M. C. Wicks, M. Salazar-Palma, and R. J. Bonneau, *Smart Antennas*, Wiley Series in Microwave and Optical Engineering, 2003.

19. Liberti, J. and T. S. Rappaport, *Smart Antennas for Wireless Communications: IS-95 and Third Generation CDMA Applications*, Prentice Hall Communication Engineering & Emerging Technologies Series.